Calibration of the Electric Field Detector for the CSES-02 satellite

G. Rebustini([1])([3]), R. Ammendola([1]), D. Badoni([1]), C. De Santis([1]),
P. Diego([2]), E. Fiorenza([2]), G. Masciantonio([1]), A. Parmentier([2]),
M. Piersanti([4]) and P. Ubertini([2])

([1]) *INFN, Sezione di Tor Vergata - Rome, Italy*
([2]) *INAF, Istituto di Astrofisica e Planetologia Spaziali - Rome 00133, Italy*
([3]) *Physics Department, University of Rome "Tor Vergata" - Rome 00133, Italy*
([4]) *Physical and Chemical Sciences Department, University of L'Aquila - L'Aquila 67100, Italy*

Summary. — The second China Seismo-Electromagnetic Satellite (CSES-02) will be equipped with the new Electric Field Detector (EFD-02), to measure the ionospheric electric field components at a Low Earth Orbit (LEO) over a wide frequency band (DC - 3.5 MHz) and with a high sensitivity ($\sim 1\ \mu$V/m). EFD-02 will measure the voltages between different pairs of probes installed at the tips of four booms deployed from the satellite. Compared to the previous similar detectors on board CSES-01 and DEMETER missions, EFD-02 has a cutting-edge sensitivity that allows to observe more thoroughly the variation in the electric field under the magnetic field conditions encountered in its orbit around the Earth.

1. – Introduction

The China Seismo-Electromagnetic Satellite (CSES) mission is meant to monitor dynamic perturbations of top-side electromagnetic field, plasma and particles of the Earth's ionosphere to study their possible correlations with the occurrence of seismic events. Another major goal of the mission is the investigation of the interaction between the solar wind and magnetosphere-ionosphere system [1]. The CSES-02 mission foresees the launch of a second satellite, scheduled by the end of 2022, with an expected lifetime of 6 years.

2. – The Electric Field Detector and its subsystems

The Electric Field Detector (EFD) measures the differences in electric potential (with respect to the spacecraft potential) between different pairs of probes mounted at the tips of 4 booms deployed at 4.5 m from the satellite. Electric field (E) components are

obtained as the difference between two probes voltages divided by their relative distance (8.3 m on average).

The main EFD parts are represented by the Electric Field Probes (EFPs) and the Electronics Box (EB). EFPs are 4 identical sensors which, housing a spherical shell placed at the end of the satellite boom, have the task of detecting the potential with high precision. The EB, placed inside the satellite, holds: the *Low Voltage Power Supply and Control* (LVPS and CTRL); *Splitter*; *Analog Processing Unit* (APU); *Digital Processing Unit* (DPU). The LVPS and CTRL manages power supply, housekeeping and TM/TC interface towards the satellite. The *Splitter* controls the switching of signals and power-supply lines of the EFPs between the hot and cold electronics. The APU makes the analog-to-digital conversion and pre-filtering of the signals. The DPU (based on a Xilinx FPGA) performs digital processing, On-Board Data Handling (OBDH), the command and control of the payload.

Compared to previous similar detectors on board CSES-01 [2] and DEMETER satellites (EFD-01, ICE, respectively), the EFD-02 signal acquisition is characterized by an improved frequency resolution, amounting to 5 different bands (ULF = 0–100 Hz, ELF = 19 Hz–2 kHz, VLF = 1–50 kHz, VLFe = 21–100 kHz, HF = 21 kHz–3.5 MHz). In addition, an increased total number of channels (for both scientific and redundancy purpose), with a better bit depth and higher frequency resolution, allows to produce clearer signals and optimize the signal to noise (S/N) ratio. EFD-02 is able to measure the electric field components over a *wide-band frequency range* (DC - 3.5 MHz) and with *high sensitivity* (about $1 \mu V/m$) in the ULF band. Finally, in EFD-02, the "Switch Matrix" allows to choose the probe pairs used for the evaluation of the 3 components of the electric field.

The APU, representing the core of the detector, performs a preliminary subdivision into 3 frequency bands (LF, MF, HF) and makes the analog-to-digital conversion. All APU channels (4 LF, 3 MF, 3 HF) withstand voltages up to ± 7.3 V at their inputs. Low noise op-amps are used for buffers and analog chains. The three HF channels are selected by a *fast mux* to use a unique HF ADC needed to respect the power consumption constraint. The ELF, VLF and VLFe bands are produced by DPU from the MF band; the LF band is further filtered by DPU to obtain the ULF band.

A 16-bit DAC generates voltages in the ± 5 V range, which are sent simultaneously to the 4 probes and then converted, through a voltage-current converter, into the bias current, which is needed to minimize the contact impedance between the probe and plasma. Then, data are sent to the DAC from the DPU board.

This current injection is also used as AC signal to determine the coupling resistance between the probe and plasma. It consists of a sine current waveform with an adjustable amplitude from a few tens to a few hundreds of nA in the ULF band. Such a signal is superimposed on the DC bias current.

3. – Performance assessment and discussion

The first integration of the EFP + APU system, hereafter System Under Test (SUT), was carried out at INFN, Roma Tor Vergata in September 2020. In order to assess the functionality and performance of the SUT, a large variety of tests (Sensitivity; Linearity; Dynamic range; Bandwidth; Signal/Noise Ratio (SNR); Power Spectral Density) have been performed both before and after DPU digital filters.

The sensitivity of the system is defined as the smallest measurable signal, in the time domain, which can be discriminated from noise. Therefore, a good estimate of the
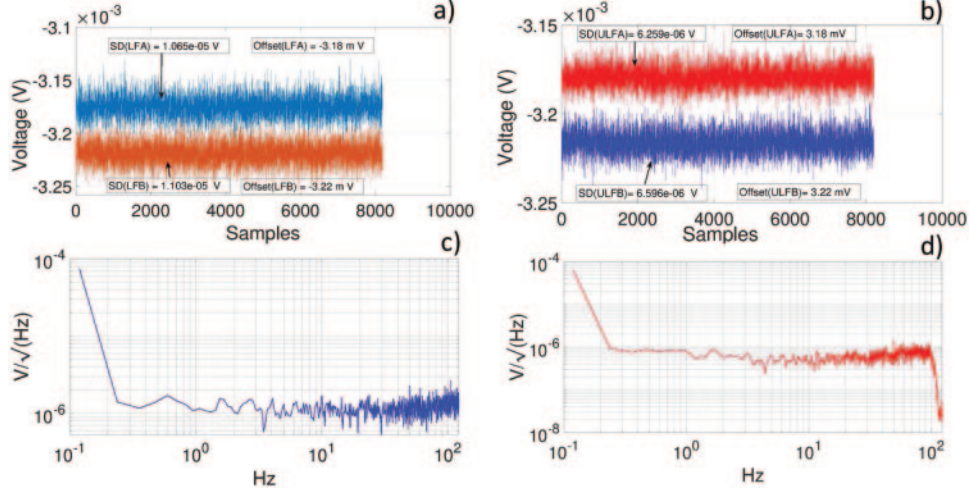
Fig. 1. – (a) Pre-filtering: SD LFA $= 10.65\,\mu$V, LFB $= 11.03\,\mu$V and offset $\approx -3\,$mV, in the LF band; (b) post filtering: SD LFA $= 6.26\,\mu$V, LFB $= 6.60\,\mu$V and offset $\approx -3\,$mV, in the ULF band; (c) NVSD, pre-filtering $\approx 1\,\mu$V/$\sqrt{\text{Hz}}$; (d) NVSD, post-filtering $\approx 600\,$nV/$\sqrt{\text{Hz}}$.

system sensitivity is provided by the electronic noise *Standard Deviation* (SD). On the other hand, in the frequency domain we use the *Noise Voltage Spectral Density* (NVSD) which is a measurement of the RMS noise voltage per square root of hertz. Panels (a) and (b) of fig. 1 show the measurement of the SD before (LF) and after (ULF) the digital filtering, respectively. Panels (c) and (d) represent the measurements of NVSD for the difference between the A/B probe pair with the inputs connected to ground, before and after the digital filtering, respectively.

The I/O signal linearity has been studied throughout the entire dynamical range and frequency band, at different frequencies for each of the 5 bands, and at different amplitude values of the input signal. This step provides both the analog to digital conversion factor matrix (volts/digit) at different amplitudes and frequencies, and the calibration of the system. Many robustness, functionality and performance tests have been successfully performed on the analog sections of EFD-02: electronic stability in a Climatic Chamber and gamma irradiation tests.

EFD-02 has been also tested in the Plasma Chamber facility at INAF-IAPS [3] to evaluate its performance in a "quasi-realistic" flight environment. Various tests have been conceived to outline the instrument capabilities in operating under different conditions possibly encountered along the spacecraft (S/C) orbit. To evaluate the effects of the magnetic field component parallel to the plasma beam (*i.e.*, the typical conditions of a Sun-synchronous orbit S/C [4]), we measured the EFD floating potential (V_f) for three magnetic field values ($B = 0.01\,$G, value of the minimum residual field, $B = 0.25\,$G and $B = 0.45\,$G), representing the ideal and the average mid-low latitude geomagnetic conditions, respectively. The other components were kept within the minimum values (*i.e.*, $B \leq 0.01$ G). Such observations were compared to the theoretical V_f values expected by the Orbit Motion Limited (OML) theory [4]. The theoretical V_f values were computed by means of plasma density and electron temperature (T_e) values retrieved from Langmuir probe measurements on board the satellite [4]. The OML expected results together with
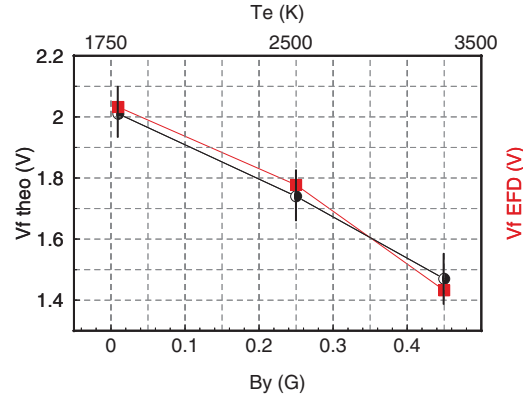
Fig. 2. – Theoretical values (black squared markers) of EFD are displayed together with the measured floating potential (red circles) for three different values of magnetic field component parallel to the plasma beam in the Plasma Chamber. The error bar amplitude of the theoretical values is obtained by the propagation of the diagnostic measurements uncertainties, while the error bar amplitude of the measured potential by EFD is obtained by the environmental noise.

the measured ones are shown in fig. 2. The observed V_f decrease for increasing B is an expected behaviour caused by the smaller electron gyro-radius and the relevant forced motion of the electrons around the probe surface which, in turn, reduces the electron saturation current ([5] and reference therein). In addition, an increased electron temperature (T_e) is observed as expected from the reduced slope of the characteristic curve of the sensors. Moreover, the V_f reduction is also coherent with the rule of thumb establishing that V_f is a few kT lower than the plasma potential V_p ([6] and references therein). Then, when V_p is constant, V_f decreases for increasing T_e (as shown in the top horizontal axis in fig. 2).

In conclusion, EFD's intrinsic noise level has been assessed to be largely lower than the environmental noise observed in the plasma chamber facility, which ensures the accurate evaluation of small perturbations in particle collection on the probe surface as the ones induced by Earth's magnetic field variations.

REFERENCES

[1] DIEGO P. *et al.*, *Instruments*, **5** (2021) 1.
[2] HUANG J. *et al.*, *Earth Planet. Phys.*, **2** (2018) 469.
[3] `http://www.iaps.inaf.it/2019/04/24/laboratorio-di-fisica-del-plasma-e-camera-del-plasma`.
[4] DIEGO P. *et al.*, *IEEE Access*, **5** (2017) 3824.
[5] CHUNG P. M., TALBOT L. and TOURYAN K. J., *Electric Probe in Stationary and Flowing Plasma: Theory and Application,* in *Applied Physics and Engineering* (Springer-Verlag) 1975, `https://doi.org/10.1007/978-3-642-65886-0`.
[6] CHEN F. F., *Langmuir Probe Diagnostic, Lecture Notes, Mini-Course on Plasma Diagnostics, IEEE-ICOPS meeting, Jeju, Korea, June 5, 2003* (IEEE) 2003.